Catalysis Letters Vol. 105, Nos. 3–4, December 2005 (© 2005)
DOI: 10.1007/s10562-005-8692-7

Water denitration over a Pd–Sn/Al_2O_3 catalyst

Jacinto Sá[a,e], Dana Gasparovicova[b], Konrad Hayek[c], Erich Halwax[d], James A. Anderson[e], and Hannelore Vinek[a,*]

[a]*Institute of Materials Chemistry, Vienna University of Technology, Veterinärplatz 1, A-1210 Vienna, Austria*
[b]*Department of Organic Technology, , Radlinskeho 9, SK-81237 Bratislava 1, Slovak Republic*
[c]*Institute of Physical Chemistry, University of Innsbruck, Innrain 52A, A-6020 Innsbruck, Austria*
[d]*Institute of Chemical Technologies and Analytics, Division of Structural Chemistry, Vienna University of Technology, Getreidemarkt 9, 164- SC, A-1060 Vienna, Austria*
[e]*Surface Chemistry and Catalysis Group, Department of Chemistry, University of Aberdeen, Meston Walk, Old Aberdeen, AB24 3UE, UK*

Received 19 April 2005; accepted 2 August 2005

Bimetallic Pd–Sn catalysts were synthesized by incipient-wetness impregnation of the metals on alumina and employed for the reduction of nitrates from aqueous solutions. The catalysts were characterized by FTIR spectroscopy of adsorbed CO, X-ray diffraction (XRD), transmission electron microscopy (TEM), and H_2 chemisorption. The influence of the metal ratio was evaluated in reaction measurements. The bimetallic Pd–Sn catalysts exhibited high selectivity for nitrate removal forming less NO_2^- and NH_4^+ than the Pd–Cu catalysts.

KEY WORDS: Pd–Sn/Al_2O_3; nitrate hydrogenation; XRD; FTIR using CO and TEM.

1. Introduction

Demand for water of good quality has increased with the increased intensity of water uses. However, excessive application of fertilizers and pesticides in agriculture can lead to leaching of nitrates, ammonium, sulphates and other harmful substances into the groundwater and hence into surface water, Nitrates, in particular (above a certain concentration), can be a danger to human health.

The quality of water intended for human consumption should have as a guide level 25 mg NO_3/L and a maximum tolerable concentration of 50 mg NO_3/L. According to the Dobris M. Assessment, compiled by the European environmental Agency in 1998 [1], it appears that 87% of agricultural areas in the EU have nitrate concentrations in groundwater above the guide level of 25 mg/L, and approximately 20% of the agricultural area exceeded the concentration of 50 mg NO_3/L. The strict legal limits imposed by the EU, i.e. 50, 0.1 and 0.5 ppm for NO_3^-, NO_2, and NH_4^+, respectively, creates an urgent need for the development of new technologies for denitration.

From an environmental point of view, the most favourable way to remove nitrates is to convert them into N_2 [2]. In order to achieve this, one potential process is the liquid phase hydrogenation over a bimetallic catalyst [2–23]. The catalysts necessary for this process must be very active because the reaction must be performed at the temperature of ground water. Moreover, a high selectivity is necessary to avoid the production of ammonium ions by over-reduction of intermediates in the stepwise nitrate hydrogenation [17]. Till now, bimetallic catalysts based on Pd have appeared to be the most promising.

It is known that supported Pd is one of the most active catalysts in the liquid phase hydrogenation of aromatic compounds [24]. The addition of a second component to a metallic catalyst is a well-known method of modifying its activity and selectivity. In the case of reduction of nitrates, the second metal (Cu, Sn, In) is needed to increase the rate of conversion of NO_3^- to NO_2^-. With Pd–Cu catalysts having the optimum metal composition, selectivity for nitrate reduction ranging from 80 to 95% can be reached [7, 8, 11, 13]. A further improvement is obtained if a nitrate reducing Pd–Cu catalyst is combined with a nitrite reducing Pd catalyst [33].

One major draw back of the catalytic reduction process is the formation of ammonia as a side product and nitrites as an intermediate. Further improvements to these catalysts are necessary to optimise their performance because of an interdependence of nitrate activity and nitrogen selectivity.

Pd–Sn supported on alumina showed higher activities and selectivities for the removal of nitrates than Pd–Cu catalysts [14], although the opposite was found when Pd–Sn was supported on titania or zirconia, Recently, Pintar *et al.* [25] reported that Pd–Sn catalysts supported on alumina exhibited significantly lower activity for nitrate removal than Pd–Cu catalysts.

Berndt *et al.* [26] and Mönnich [27] studied Pd–Sn catalysts supported on alumina by FTIR and ^{119}Sn–Mössbauer spectroscopy. Their catalysts contained both Pd–Sn and pure Pd ensembles, which coexisted on

* To whom correspondence should be addressed.
E-mail: vinek@tuwien.ac.at; http//www.imc.tuwien.ac.at/catalysis

1011-372X/05/1200–0209/0

the catalysts. Furthermore, ensembles of Pd–Sn containing alloys with different composition and Sn^{2+} and Sn^{4+} species where identified. The alloys were suggested to be the active species, whereas Sn^{4+} species were inactive and Sn^{2+} species were suspected of acting as inhibitors.

The aim of this work was to compare the activity and selectivity for nitrate reduction with the surface properties of bimetallic Pd–Sn catalysts supported on alumina. XRD, TEM and CO adsorption followed by IR measurements was used to characterize the catalysts.

2. Experimental

2.1. Catalyst synthesis

γ–Al_2O_3 (Sigma Aldrich ALOX506C; BET specific surface area of 155 m^2/g, average pore diameter 5.8 nm, particle size 150 mesh) was employed as a carrier of the active components. The metal salts used for impregnation ($Pd(NO_3)_2 \cdot 2H_2O$, $SnCl_2$and $Cu(NO_3)_2 \cdot 3H_2O$) were supplied by Sigma-Aldrich.

Bimetallic catalysts were prepared by incipient-wetness impregnation of the support material with the metal salts. These salts were dissolved in 0.7 mL water/g catalyst, which corresponds to the pore volume of the support. In a first step, the support was impregnated with tin chloride (dissolved in a mixture of water acetone (6:1)), dried overnight at 100 °C and calcined at 500 °C for 1 h, and then impregnated with Pd nitrate. The solids obtained were dried overnight at 100 °C, calcined in air at 500 °C for 3 h and finally reduced in a hydrogen atmosphere for 1 h at 500 °C. The theoretical amount of Pd was 5 wt% throughout, while the amount of Sn was varied from 1 to 2.5 wt%.

The same procedure was adopted in order to synthesize a Pd–Cu/γ-Al_2O_3 catalyst with a Pd/Cu wt% equal to 5/1.25. A loading of 5 wt% Pd was chosen to match that used by Vorlop and co-workers [3–9] to prepare PdCu and PdSn catalysts for nitrate abatement.

2.2. Catalyst characterisation

ICP-MS (Inductively Coupled Plasma Mass Spectroscopy) measurements were carried out in order to determine the Pd and Sn content of the catalysts. After dissolution of the samples in *aqua regia* and dilution with distilled water, the catalysts were analysed using a SpectroMass 2000 working at a generator power of 1350 W and with the nebulizer at 1050mL/min. The element isotopes determined by ICP-MS were ^{105}Pd, ^{106}Pd, ^{118}Sn and ^{120}Sn. The isotopes used for the calculations were ^{105}Pd and ^{120}Sn. Analysis of Cu loading was achieved by AAS (Atomic Absorbance Spectroscopy) on a Perkin–Elmer 2280.

The surface areas of the catalysts were determined with a Quantasorb apparatus using the BET method (N_2, 77 K) [28]. H_2 chemisorption was measured at 80 °C on the bimetallic Pd–Sn catalysts to obtain the accessible Pd metal fraction. The catalysts were previously reduced at 500 °C in pure H_2 for 2 h and degassed at 400 °C for 2 h in N_2. Degasification was applied to remove the hydrogen that was adsorbed during the reduction. The measurements were carried out at 80 °C to avoid the formation of Pd β-hydride. According to Mélendrez *et al.* [29], the presence of Pd β-hydride is avoided when the measurement are performed above 70 °C. Bastista *et al.* [30] suggest that Pd β-hydride decomposition occurs at 39 °C.

FTIR measurements were carried out on a Bruker IFS 28 instrument using a resolution of 4 cm^{-1}. The spectrometer cell was connected to a vacuum system working in the 10^{-6} mbar range and to a heating system. The cell was prepared for *in situ* pre-treatments of samples and adsorption of gases. The samples were pressed into self-supporting wafers that where placed inside a ring furnace in the vacuum cell. The catalysts were reduced *in situ* at 500 °C in $H_2$for 1 h. The cell was then evacuated for using the same period of time and temperature as used for the reduction. The samples were exposed to 50 mbar CO at 25 °C. The spectra presented are normalized by weight.

XRD patterns were measured on a Philips X'Pert PRO diffractometer (Bragg–Brentano θ/θ-geometry type; CuKα radiation, graphite (002) monochromator, continuous scans in the region $2\theta = 5$–80°, step size 0.02° with a scan rate of 5 s/step). Crystalline phases were identified using the Powder Diffraction File [31].

The morphology was studied by TEM measurements collected on a Zeiss EM10C.

2.3. Catalytic test

The catalytic performances of the catalysts were tested in a slurry thermostated batch reactor with a capacity of 1 L equipped with a mechanical glass stirrer. In a typical run, 350 mg of the catalyst was charged into the reactor containing 0.73 L of distilled water. The content of the reactor was flushed for 60 min with CO_2 and H_2. The reaction was initiated by addition of a 20 mL solution of KNO_3 (Merck) in order to achieve a concentration of 100 ppm of nitrates. A constant feed of 90 mL/min for CO_2 to adjust the pH and H_2 was maintained using mass flow controllers. The reactions were carried out at atmospheric pressure, at 25 °C and using a stirring rate of 500 rpm. The total time of a typical kinetic run was 4 h.

Degradation of nitrates and formation of nitrites and ammonia were measured at constant time intervals by a colorimetric test supplied by Merck.

For the calculation of nitrate removal activity, the slope of the initial linear part of the concentration-time curve was used, which reflects the maximum activity.

3. Results and discussion

3.1. Catalyst characterization

A summary of the amounts of Pd, Sn and Cu determined by ICP-MS or AAS, the specific surface areas and the μmoles of hydrogen chemisorbed on the catalysts is reported in Table 1. The BET surface areas of the catalysts after impregnation are approximately constant when compared with the initial support.

The measured tin loadings were less than the nominal values, which could be due to the incomplete digestion of the metal by the *aqua regia* but also due to the assay of the precursor salt used and the low solubility of the chloride salt. The concentration of tin used in the discussion is that measured by ICP-MS.

Bimetallic Pd catalysts can be prepared by non-selective deposition in which there is no interaction between Pd and the second metal during the deposition process and also by a selective deposition process in which one precursor is selectively deposited onto the metallic particles of the other component [32]. With the non-selective deposition such as wet impregnation, close contact between the two components is not always achieved in the final reduced catalyst, and a wide range of mono- and bi-metallic particles of different compositions can exist on the support surface.

Table 1
Resume of metal loadings, surface area and H_2 chemisorbed

Catalyst	Pd wt%	M wt%	Pd:M atomic ratio	Surface area m^2/g	*n*H2 adsorbed (μmol/gcat)
Sn_Al	–	0.25	–	–	0
PdSn1	4.5	0.19	1:0.035	153	62
PdSn2	5.1	0.34	1:0.060	143	88
PdSn3	4.4	1.21	1:0.244	145	77
PdCu	5.0	1.25	1:0.417	148	–

M = Sn or Cu.

One way of minimizing the heterogeneity of the metal particles is by applying a reduction procedure at high temperatures. This normally leads to sintering of the metals and alloy formation, The resultant material is generally characterized by large bimetallic particles with a higher degree of homogeneity with respect to the particle size distribution. In order to validate this assumption, TEM and XRD measurements were carried out.

TEM investigations showed a tin metal particle size distribution between 10 and 20 nm (figure 1a) for the monometallic catalyst Sn_Al. The particles size increased up to 80 nm for the bimetallic catalyst PdSn1 (figure 1b). The TEM images indicate an increase in particle size, but the degree of homogeneity is still rather poor.

It is known that alloy formation occurs readily when palladium and copper are supported on alumina and reduced at higher temperatures [27, 33]. XRD measurements were carried out in order to check whether reduction of the Pd–Sn catalysts at 500 °C leads to alloy formation.

The X-ray diffraction patterns of PdSn3 calcined at 500 °C and then reduced at 500 °C are shown in figure 2. In the calcined sample only PdO and Al_2O_3 give rise to diffraction lines whereas in the reduced sample, metallic palladium and lines assigned to paolovite ('Pd_2Sn') and 'Pd_3Sn' were observed. The presence of 'Pd_2Sn' and 'Pd_3Sn' species confirms that alloy formation had taken place whereas the lines related to metallic palladium provide evidence for the presence of Pd excess. From the stoichiometry of the alloys produced and the atomic ratio of the starting reagents, palladium would be expected to be in excess. The formation of crystalline 'Pd_2Sn' and 'Pd_3Sn' as well as the presence of metallic palladium were observed for all Pd–Sn catalysts studied in this work, as shown in figure 2. From the diffractograms of the reduced catalysts (figure 3), it can be concluded that the excess palladium is present in the metallic state.

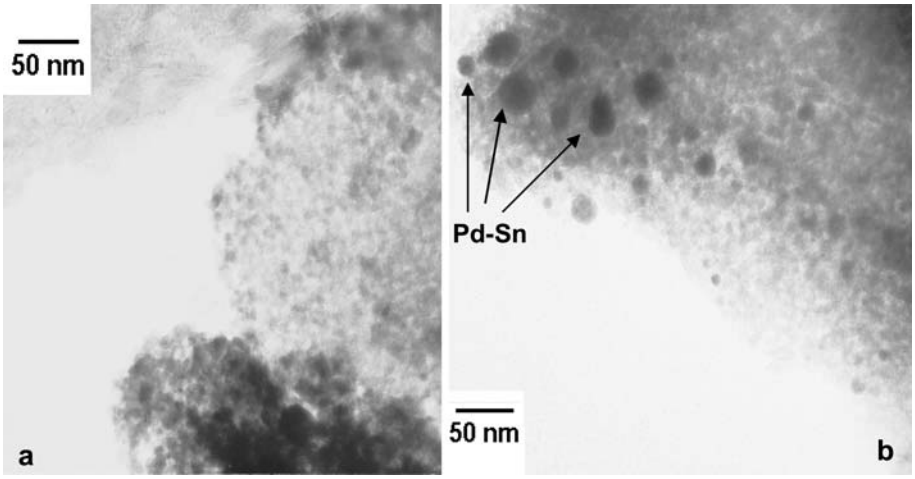

Figure 1. TEM images of the tin catalysts. (a) Sn_Al, (b) PdSn1.

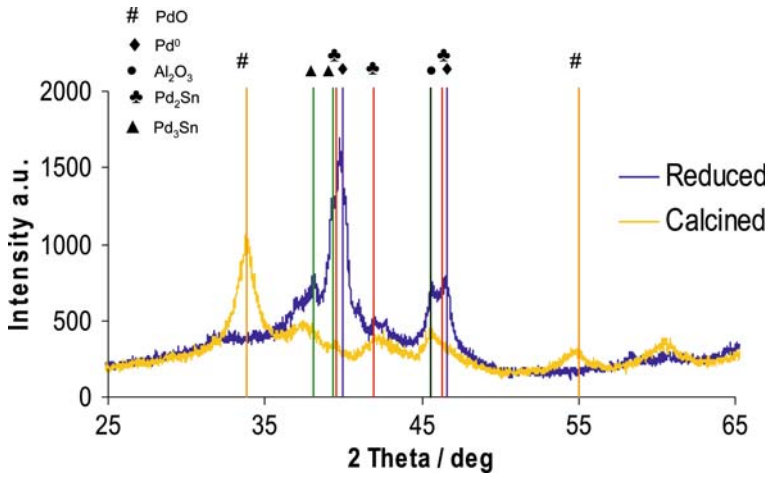

Figure 2. Comparative XRD profiles of PdSn3 catalyst in calcined and reduced states.

To investigate the oxidation states and the accessibility of the exposed metals in the Pd–Sn catalysts, CO adsorption was followed by IR spectroscopy. For Sn_Al one band is observed at 2199 cm^{-1} (not shown), which can be ascribed either to adsorption of CO on Sn^{4+} [34] or to CO interacting with $A1^{3+}$ on the alumina surface [35]. The band disappeared after evacuation of the cell at 25 °C. Silva *et al.* [36], in H_2-TPR experiments, reported a reduction temperature of 510 °C for particles of tin oxide supported on alumina was (Sn wt% = 4.7). Based on this information, it can be expected that tin particles are present in their lower oxidation states of Sn(II) and Sn(0), predominantly, and that the measured band is therefore related to CO interacting with $A1^{3+}$ species. This might explain that under the conditions used no IR band related to CO chemisorbed on tin species was observable.

Results of FTIR experiments of CO adsorption on PdSn1 and PdSn2 are shown in figure 4a and 4b, respectively. The band around 2151 cm^{-1} is assigned to CO adsorption on residual Pd^{2+} species [37], since interaction of CO with Sn^{2+} at room temperature is very weak and does not produce measurable bands under these experiments conditions. Chloride ions, from the tin precursor, which are not fully removed by the reduction procedure, could stabilize these palladium ions [35]. The band decreased upon evacuation but did not disappear.

The band at around 2100 cm^{-1} is assigned to CO linearly bonded to metallic Pd. The intensity of this band decreased markedly upon evacuation at 298 K. Bands at lower wave numbers are attributed to bridged CO species adsorbed at different exposed metallic Pd facets. After evacuation at 298 K, the band at around 1988 cm^{-1} decreased in intensity and shifted to lower wave numbers, whereas the carbonyl species giving the band near 1930 cm^{-1} were unaffected. Sales *et al.* [35] observed only one very broad band centred at 1980 cm^{-1} for Pd–

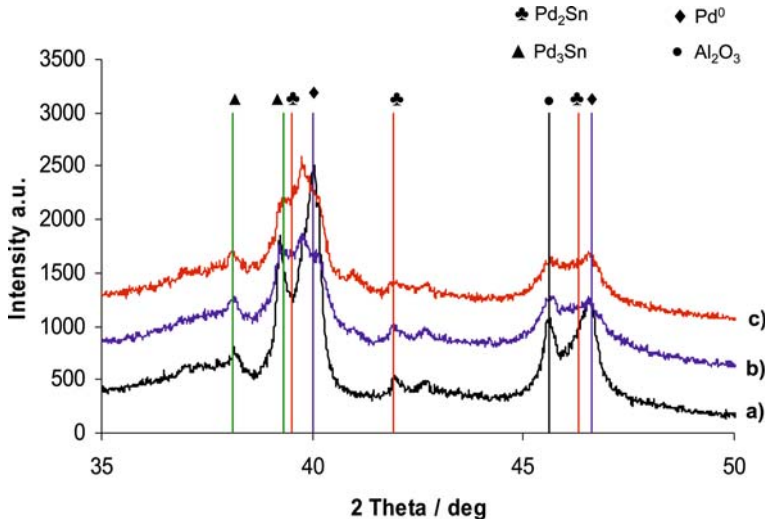

Figure 3. XRD profiles of all Pd–Sn catalysts after reduction. (a) PdSn1, (b) PdSn2, (c) PdSn3.

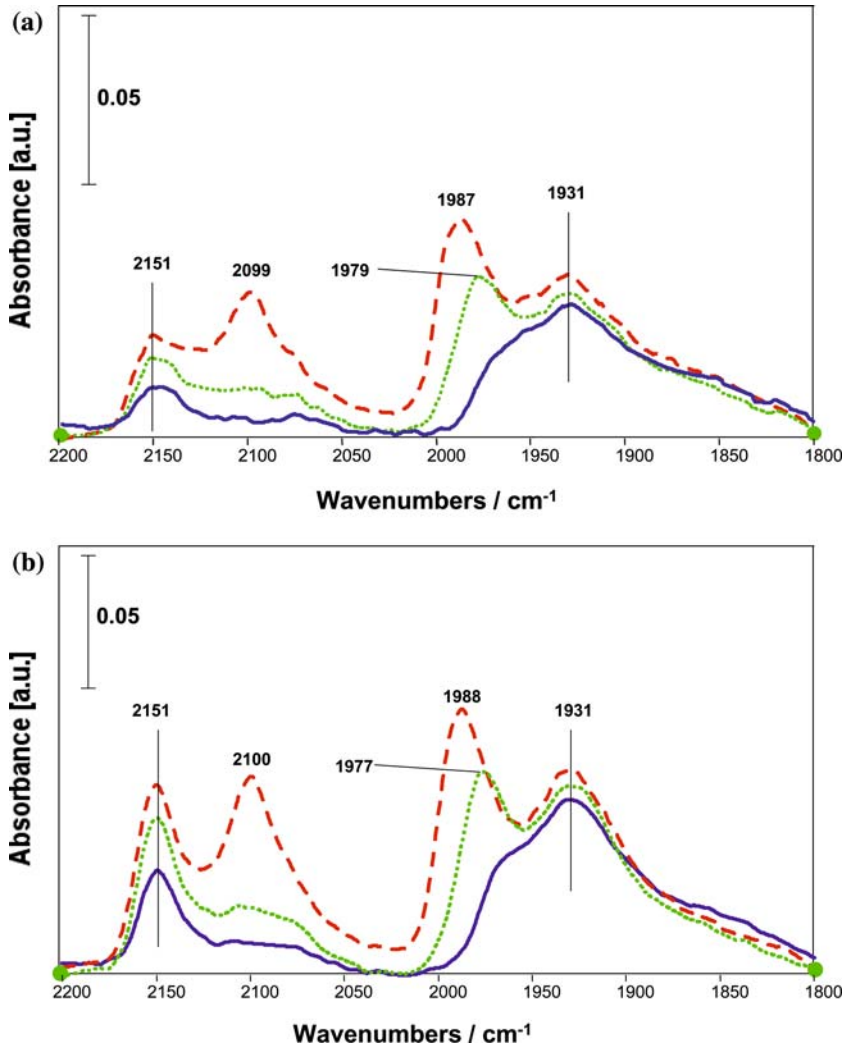

Figure 4. IR spectra of CO interaction with PdSn catalysts after reduction in hydrogen for 1 h at 500 °C and evacuation at 500 °C for 1 h. (a) PdSn1; (b) PdSn2.– –CO adsorption, •··• CO interaction after 1 min evacuation, —CO retained after 1 h evacuation.

Sn supported on alumina catalysts, a feature which they attributed this feature to three different types of bridged CO species adsorbed on metallic palladium. The band near 1930 cm^{-1}in the spectra (figure 4 a, b) are ascribed to compressed bridged CO species adsorbed on high index planes of metallic Pd or to CO in threefold sites on Pd [35]. Sales *et al*. [35] observed this band at 1930 cm^{-1} only for monometallic Pd/Al_2O_3 catalysts. The presence of bridged adsorbed CO on Pd–Sn catalysts suggests the presence of pure Pd ensembles in addition to bimetallic sites, a suggestion also supported by the XRD patterns exhibiting diffraction lines related to pure Pd, consistent with literature reports [26, 27].

After evacuation at room temperature, the bands around 1988 and 2100 cm^{-1} related mainly to Pd–Sn ensembles decreased sharply in intensity and shifted to lower wave numbers, This behaviour can be explained by the influence of Sn, which weakens the CO adsorption strength [35, 38]. This can be due to an electronic effect and/or dilution effect. Bastein *et al*. [38], using the Isotopic Dilution Method [39], report that the red shift in the absorption band frequency of CO adsorbed on Pt when alloyed with Sn can be (almost) fully understood in terms of a dilution effect. Upon alloying, the distance between the CO molecules on Pt atoms has been observed to increase, which consequently gives reduced dipole–dipole coupling between CO molecules. Sales *et al*. [35] suggested similar behaviour when Pd was used instead of Pt.

In figure 5 the spectra of CO on Pd–Sn1, 2 and 3 are compared. Since the spectra are normalized with respect to sample masses, the intensities of the bands allow an estimation of the relative abundance of Pd and Pd–Sn surface ensembles. It can be inferred from figure 5 that the amount of surface palladium first increases with increase in the loading of tin and then decreases. This behaviour is specially pronounced for the bands related with the Pd–Sn ensembles (bands at around 1988 and 2100 cm^{-1}). The increase in band intensity and symmetry from PdSn1 to PdSn2 is also followed by small a red shift in frequency. This suggests that the bimetallic

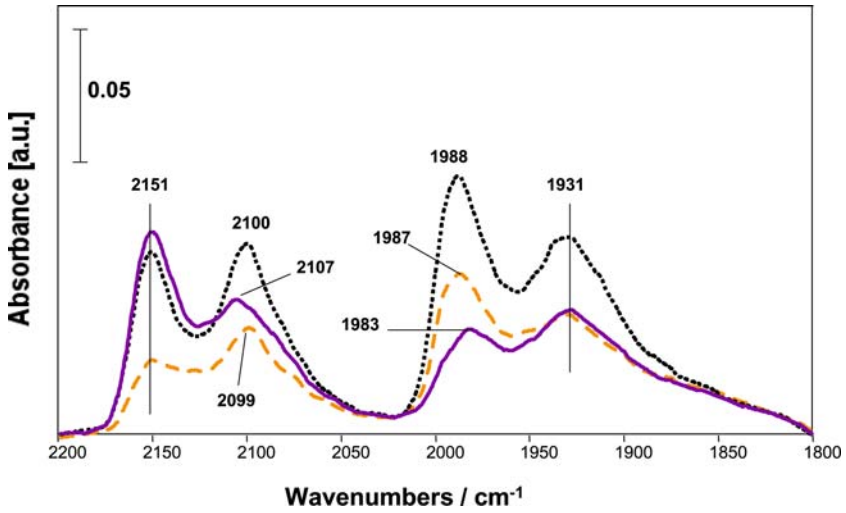

Figure 5. Mass normalized FTIR spectra of CO adsorption on Pd–Sn samples after pretreatment at 500 °C with hydrogen for 1 h and evacuation at 500 °C for 1 h, – – – PdSnl,PdSn2, ——PdSn3.

ensembles formed are more homogeneous, as the presence of tin reduces the dipolar coupling interaction between the neighbouring adsorbed CO molecules [38]. This is consistent with the view that Pt in Pt–Sn alloy is less electron deficient than Pt alone [40, 41], and would suggest that an electronic effect of adding Sn should contribute to a red shift in ν_{co}

After reaching the maximum for PdSn2, tin is expected to segregate at the surface of the metallic particles forming amorphous islands of monometallic tin, which lead to a decrease in the concentration of exposed Pd [42]. The band related to bridged CO on Pd of the catalysts PdSn3 is slight shifted towards lower frequencies, as a function of the one observed for the catalysts PdSn1 and PdSn2, suggesting that some of the segregated tin came from the preformed PdSn ensembles.

It is also possible to confine from figure 5 that the existence of the Pd^{2+} species is a consequence of the presence of Cl^- from the tin precursor since the band intensity due to CO adsorbed at these sites increases with increasing tin loading.

3.2. Catalytic test reactions

The activities and selectivities of the different catalysts are summarized in Table 2. A typical course of the changes of nitrate, nitrite and ammonium ion concentrations during a batch experiment is demonstrated in figures 6–8. The depletion of nitrates follows approximately a first order decay. The amounts of intermediate nitrites are rather small over the Pd–Sn catalysts in comparison with the amount observed over Pd–Cu (figure 7), while ammonium forms throughout the course of the reaction. The final amount of ammonium is a good parameter to evaluate the selectivity of the catalysts.

Table 2
Activity and selectivity of the different catalysts

Catalyst	Activity for nitrate reduction (μmol/(min gcat))	Final $[NO_2^-]$ (ppm)	Final $[NH_4^+]$ (ppm)	Selectivity towards N_2 (mol %)
PdSn1	41	0.0	4.7	84
PdSn2	53	0.0	4.0	86
PdSn3	39	0.0	3.4	88
PdCu	50	0.0	6.8	77

An active catalyst for nitrate reduction should have a certain number of bimetallic sites as well as monometallic Pd sites. Reduction of nitrates to nitrites can be achieved at the bimetallic sites by an electron transfer to the adsorbed nitrate followed by a subsequent regeneration of the sites by hydrogen. Nitrites may then be reduced to nitrogen or overreduced to ammonia at monometallic Pd sites [32].

100% nitrate conversion was reached within 180 min for all studied bimetallic catalysts. The most active catalysts were PdSn2 and PdCu. The activity of Pd–Sn catalysts was observed to vary as a function of the tin content (Table 2). The profiles show a typical volcano shape curve [43, 44]. The activity increases initially with increasing tin loading, then reaches a maximum with a Sn loading of around 0.34 wt%, and decreases again for higher loadings.

Hydrogen chernisorption data (Table 1) suggest that direct chemisorption of hydrogen at bimetallic ensembles is unlikely to occur; therefore the amount of chemisorbed hydrogen can be used as a direct measure of surface Pd. In figure 9 the activity and the amount of adsorbed hydrogen are plotted against the ratio of the metals in the bimetallic Pd–Sn catalysts. As one can see, the two curves show very similar trends, At first the nitrate reduction is promoted by an increasing generation of bimetallic sites, which are the active sites for adsorbing and activating the nitrate ions. With further

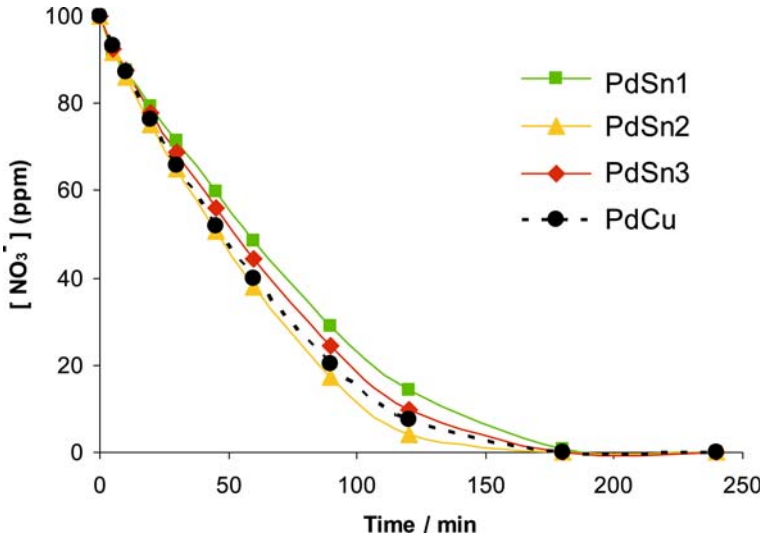

Figure 6. Nitrate conversion as a function of time.

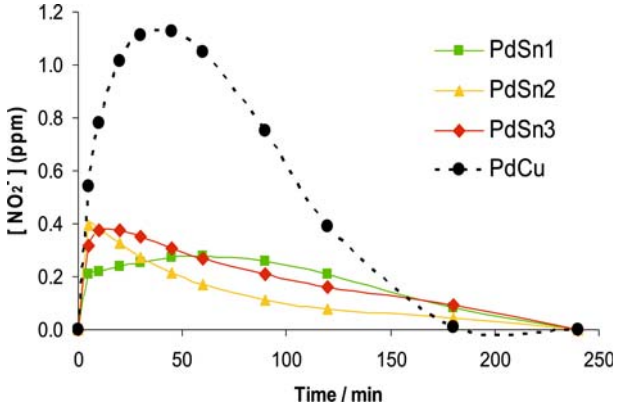

Figure 7. Nitrite formation as a function of time.

tin loading, the surface of the metal particles becomes too rich in tin. Obviously, an optimum ratio of bimetallic to monometallic domains on the surface of the catalyst particles would be necessary to obtain activity, since the monometallic palladium sites will act to provide hydrogen atoms, essential to keep the catalyst active.

The influence of tin on the activity of the PdSn catalysts may be interpreted in terms of an electronic effect caused by the tin on the Pd metal particles. Burch [45] has concluded that the addition of Sn to Pt/Al_2O_3 catalysts could make Pt either electron deficient *via* interaction with Sn (II) ions on the alumina, or electron rich *via* formation of a solid solution of Sn (0) in Pt. Therefore Sn (0) should act as a promoter for the reduction reaction whereas Sn (II) would be expected to act as an inhibitor. This is consistent with proposals put forward by Berndt *et al.* [33]. The overall activities observed are therefore a delicate balance between the amounts on tin present in its various oxidation states

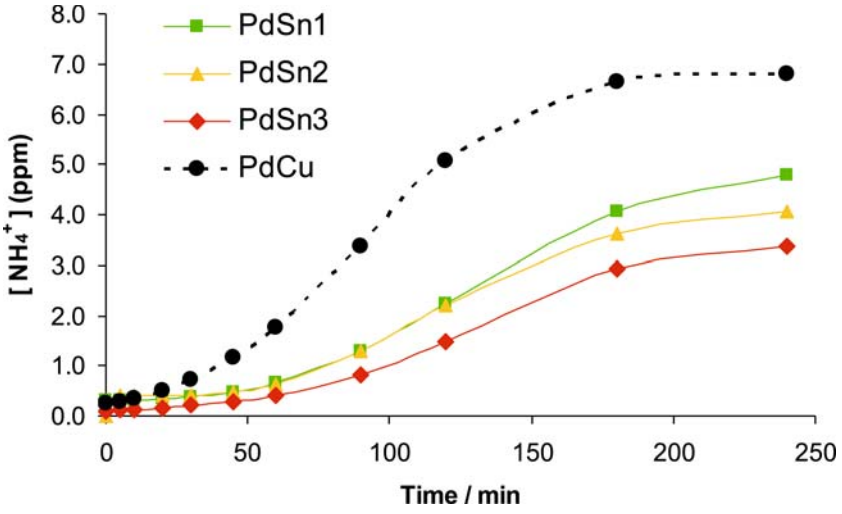

Figure 8. Ammonium formation as a function of time.

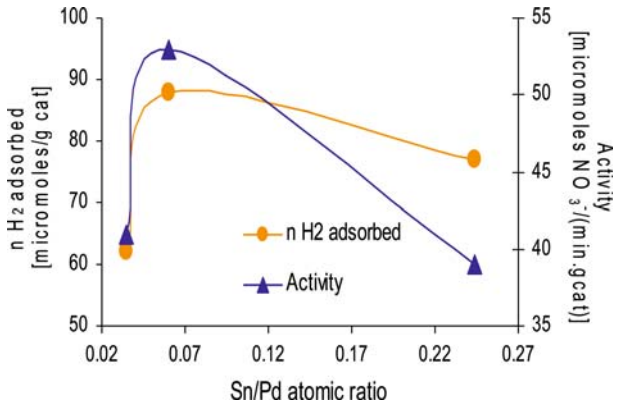

Figure 9. Relationship between activity of nitrate conversion and chemisorbed hydrogen as a function of Sn/Pd atomic ratio.

and the blocking effect of Sn atoms on Pd sites that are otherwise active for the supply of hydrogen atoms.

It can be inferred from figure 5that the selectivity of the catalysts to NH_4^+ follows the same trend as the intensity of the band at 1930 cm^{-1}, that is the band due to the interaction of CO with the high index planes of Pd. Yoshinaga et al. [46] have suggested that it is the reduction of NO that gives ammonium, which occurs at isolated atom sites which have a higher hydrogenation power than sites which are part of extended ensembles of atoms. Among these sites, the atoms are located on the high index-planes. It should be mentioned that NO has been postulated as being a potential intermediate in the reduction sequence of nitrites towards nitrogen or ammonium [10, 17].

4. Conclusions

Pd–Sn bimetallic catalysts have on their surfaces ensembles of alloyed Pd–Sn and pure Pd. Both Pd and PdSn particles were identified by XRD. The activity of the catalysts for nitrate reduction is strongly dependent on the ratio of the two described ensembles. Pd–Sn catalysts show a greater selectivity for N_2 than Pd–Cu where the latter exhibits both high ammonium and nitrite formation rates. The promotional effect of Sn on Pd shows sensitivity to the Sn/Pd ratio that determines the relative amounts of Sn^0 (promoter) and Sn^{2+} (inhibitor) and also the number of active Pd atoms, which are blocked by Sn^0 in the PdSn ensembles.

Acknowledgments

The work was supported by the 'Found zur Förderung der Wissenschaftlichen Forschung' of Austria under Project P14 972. The authors thank the group of Professor Jörg Feldmann, especially Dr Andrea Raab (University of Aberdeen), for the time provided and help in performing the ICP-MS measurements.

References

[1] http://reports.eea.eu.int.
[2] A. Corma, A.E. Palomares, F. Rey and J.G. Prato, Catal 227 (2004) 561.
[3] K.D. Vorlop, T. Tacke, M. Sell, G. Strauss, DE 3830850 A1, European Patent Office, 10 September, 1988.
[4] T. Tacke, K.-D. Vorlop, Dechema Biotechnology Conferences, Vol. 3, VCH, Weinheim, 1989, 1007.
[5] K.-D. Vorlop and T. Tacke, Chem. Ing. Tech. 61 (1989) 836.
[6] K.-D. Vorlop, S. Hörold and K. Pohlandt, Chem Ing. Technol. 64 (1992) 82.
[7] S. Hörold, T. Vorlop, K.D. Tacke and M. Sell, Catal. Today 17 (1993) 21.
[8] T. Tacke and K.-D. Vorlop, Chem Ing. Technol. 65 (1993) 1500.
[9] S. Hörold, T. Tacke and K.-D. Vorlop, Environ. Technol. 14 (1993) 21.
[10] A. Pintar, J. Batista, J. Levec and T. Kajiuchi, Appl. Catal. B 11 (1996) 81.
[11] A. Pintar, G. Bercic and J. Levec, AIChE J. 44 (1998) 2281.
[12] U. Prüsse and K.-D. Vorlop, Catal. Today 55 (2000) 79.
[13] A.J. Lecloux, Catal. Today 53 (1999) 23.
[14] G. Strukul, R. Gavagnin, F. Pinna, E. Modaferri, S. Perathoner, G. Centi, M. Marella and M. Tomaselli, Catal. Today 55 (2000) 137.
[15] F. Deganello, L.F. Liotta, A.M. Macaluso, A. Venezia and G. Deganello, Appl. Catal. B 24 (2000) 265.
[16] F. Epron, F. Gauthard, C. Pinéda and J. Barbier, J. Catal. 198 (2001) 309.
[17] J. Wärna, I. Turunen, T. Salmi and T. Maunula, Chem. Eng. Sci. 49 (1994) 5763.
[18] S. Naïto and M. Tanimoto, J. Catal. 119 (1989) 224.
[19] F. Epron, F. Gauthard and J. Barbier, Appl. Catal. A 237 (2002) 253.
[20] S. Kerkeni, E. Lamy-Pitara and J. Barbier, Catal. Today 75 (2002) 35.
[21] F. Epron, F. Gauthard and J. Barbier, J. Catal. 206 (2002) 363.
[22] R. Gavagnin, L. Biasetto, F. Pinna and G. Strukul, Appl. Catal. B 38 (2002) 91.
[23] A. Pintar, Catal. Today 79 (2003) 1.
[24] A. Benedetti, G. Fagherazzi, F. Pinna, G. Rampazzo, M. Selva and G. Strukul, Catal. Lett. 10 (1991) 215.
[25] A. Pintar, J. Batista and I. Musevic, Appl. Catal. B 52 (2004) 49.
[26] H. Berndt, I. Monnich, B. Lücke and M. Menzel, Appl. Catal. B 30 (2001) 111.
[27] I. Mönnich, Ph.D. Thesis, University Oldenburg, Germany, (2000).
[28] S. Brunauer, P.H. Emmet and E. Teller, J. Am. Chem. Soc. 60 (2000) 309.
[29] R. Mélendrez, G. Del Angel, V. Bertin, M.A. Valenzuela and J. Barbier, J. Mol. Catal. A 157 (2000) 143.
[30] J. Batista, A. Pintar, D. Mandrino, M. Jenko and V. Martin, Appl. Catal. A 206 (2001) 113.
[31] International Centre for Diffraction Data, Newtown Square, PA/USA (1996), Commercial Database.
[32] J. Sá and H. Vinek, Appl. Catal. B 57 (2004) 245.
[33] H. Berndt, I. Mönnich, P. Druska and B. LückeBook of Abstracts of the 30., Jahrestreffen Deutscher Katalytiker, Eiseenach 19–21 March (1997) 135.
[34] D. Amalric-Popescu and F. Bozon-Verduraz, Catal. Today 70 (2001) 139.
[35] E.A. Sales, J. Jove, M.J. Mendes and F. Bozon-Verduraz, J. Catalysis 195 (2000) 88.
[36] A.M. Silva, O.A.A. Santos, M.J. Mendes, E. Jordão and M.A. Fraga, Appl. Catal. A 241 (2003) 155.
[37] K.I. Hadjiivanov and G.N. Vayssilov, Adv. Catal. 47 (2002) 308.
[38] A.G.T.M. Bastein, F.J.C.M. Toolenaar and V. Ponec, J. Catal. 90 (1984) 88.

[39] F. Stoop, F.J.C.M. Toolenaar and V. Ponec, J. Catal. 73 (1982) 50.
[40] B. Shi and B.H. Davis, J. Catal. 157 (1995) 626.
[41] R. Srinivasan and B.H. Davis, J. Mol. Catal. 88 (1994) 491.
[42] G.J. Arteaga, J.A. Anderson, S.M. Becker and C.H. Rochester, J. Mol. Catal. A 145 (1999) 183.
[43] Bond G.C. Heterogeneous Catalysis – Principles and Applications, 2nd ed. (Oxford University Press, 62).
[44] P.W. Atkins, Physical Chemistry, 4th ed. (Oxford University Press, 898).
[45] R. Burch, J. Catal. 51 (1981) 348.
[46] Y. Yoshinaga, T. Akita, I. Mikami and T. Okuhara, J. Catal. 207 (2002) 37.